Presented at the 35th IEEE Photovoltaic Specialists Conference, June 20-25, 2010, Hawaii, USA

LIGHT MANAGEMENT FOR REDUCTION OF BUS BAR AND GRIDLINE SHADOWING IN PHOTOVOLTAIC MODULES

J. Jaus[1], H. Pantsar[2], J. Eckert[1], M. Duell[1], H. Herfurth[2] and D. Doble[1]
[1]*Fraunhofer Center for Sustainable Energy Systems, 25 1ST ST Suite 101, Cambridge, MA, 02141, USA*
[2]*Fraunhofer Center for Laser Technology, 46025 Port Street, Plymouth, MI, 48170, USA*
Corresponding Author: Dan Doble, ddoble@fraunhofer.org

ABSTRACT

Solar cells used in photovoltaic (PV) crystalline silicon modules commonly feature grid fingers and bus bars as front contacts. The grid fingers and bus bars partially block the sunlight from reaching the semiconductor layers of a solar cell and therefore reduce the efficiency of a solar module. In this paper, we present experimental results of different technologies to reduce the shadowing effect that bus bars and grid fingers impose. We focus on two technologies that can be easily integrated into standard PV module technology and help to increase the module's efficiency. In the first technology, a laser is used to create a scattering pattern on the front glass of the module. This pattern directs light away from the bus bars and grid fingers. In the second technology, the bus wires are coated with a diffuse reflective coating. The sunlight is diffusely reflected at this coating. A part of it is reflected at such angles that internal reflection at the front surface of the cover glass occurs. From there the light is reflected back to the solar cell and contributes to the generated photocurrent.

INTRODUCTION

Photovoltaic modules with crystalline silicon (c-Si) solar cells are the dominating technology today in the PV industry. To collect the charge carriers generated in the silicon material, highly conductive metals such as aluminium or silver are deposited on the front and on the backside of the solar cell. As the metal deposited on the front side shields the silicon from the solar radiation, the area coverage of the front metallization must be kept to a minimum in order to keep shadowing losses low. To be most effective in current collection, the front metallization is deposited in the form of closely spaced grid fingers. The width of the grid finger is determined by tradeoffs between electrical resistance, emitter sheet resistance and shading as well as restrictions imposed by the metal deposition process. An industry-standard 155 x 155 mm² solar cell with screen printed front side grid as used in our experiments has a finger width of 150 µm. With grid fingers spaced at a distance of 2.2 mm, this leads to a shaded area of 6.8 % of total cell size. The grid fingers lead to bus bars which collect the current from the grid fingers. To provide sufficient conductivity, the bus bars are much wider than the grid fingers – in the case of the cells we conducted used two bus bars with each 2 mm width lead to a shading loss of 2.6% in a 155x155 mm² cell.

The standard interconnection technology for c-Si modules is based on the use of a string ribbon, which connects the front side bus bars of one cell to the backside metallization of the adjacent cell. This string ribbon is made of a metal (e.g. copper) coated with a surface suitable for soldering, e.g. tin. During the interconnection process, the solderable metal is heated above its liquidus temperature and forms a solder joint with the bus bar. In a final step, the cell strings are laminated between two layers of an encapsulating polymer (typically ethylene vinyl acetate (EVA)), with a glass plate on top and a white back sheet on the bottom of the module.
The metallic surface of the grid fingers and the bus bars reflects a part of the incoming light, the other part is absorbed. As a result of this, the light which hits the grid fingers and bus bars is lost[1].
The goal of the work in this paper is to reduce the losses associated with the shading caused by string ribbons and grid fingers.

LOCAL DIFFUSER ON FRONT GLASS

The principle of the locally diffusing surface on the front side glass is to minimize direct sunlight on the metalized areas such as bus bars and grid fingers. The working principle is explained in Fig. 1.

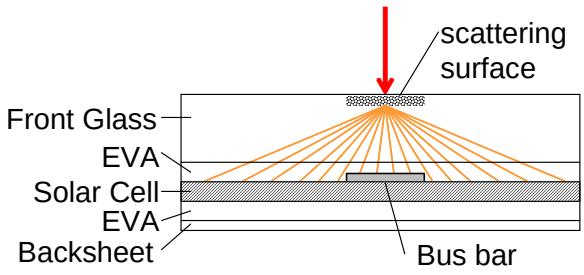

Fig. 1: Working principle of a local scattering surface. A scattering surface is created on the front side of the module's cover glass straight above metalized areas such as bus bars and grid fingers. The (perpendicularly)

[1] An exception to this can occur for non-flat grid fingers or scattering grid finger surfaces as discussed below.

incoming light is diffusely scattered at a local scattering surface so that only a small fraction of the light impinges on the bus bar. The rest is directed away from the bus bars and contributes to the photocurrent.

As shown in Fig. 1, this technology only works well if the roughened surface is directly adjacent to the metalized area and the light is impinging vertically on the module. To assure this perpendicular insulation, the modules must be mounted on a two-axis sun tracker.
For the manufacturing of the scattering surface on the module front glass, we use a 266 nm laser beam. A vision system detects the exact position of the solar cell for increased position accuracy of the process. The result of this processing is shown in **Fig. 2**.

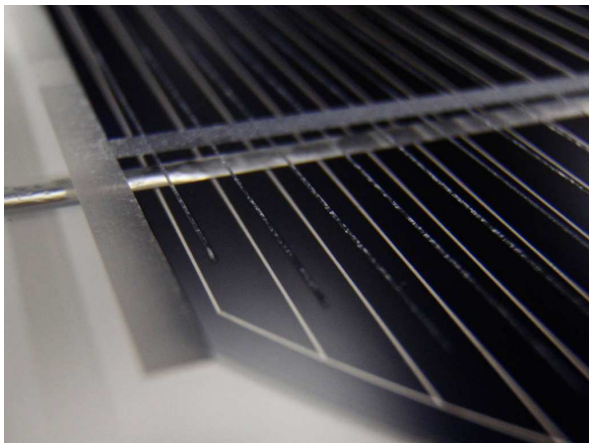

Fig. 2: *Scattering surface on a solar module on the topside of the cover glass, manufactured with a UV-Laser. The scattering structure is covers all non-active areas, such as the bus bars, grid fingers and a part of the free space between two cells.*

To determine the influence of the local diffuser surface, we manufactured mini-modules consisting of one monocrystalline 155x155 mm^2 solar cell laminated in EVA with a low iron front glass and PVF/PET/EVA back sheet. We manufactured four identical modules. Two of these were subsequently processed with the 266 nm laser to apply a local diffuser above the grid fingers and bus bars. The other two modules served as reference modules. In addition to the processing of the roughening of the glass above the grid fingers and the bus bars, a 2 mm wide perimeter area around the solar cell was processed with the laser in order to represent the effect related the cell-cell spacing in solar modules. The roughening step can also help to divert away from these areas and is therefore included in the roughening process. The electrical properties (short circuit current I_{sc}, open circuit voltage V_{oc}, efficiency σ, fill factor FF) of all four modules were measured in a Pasan 3B solar simulator with low light divergence (±1º) to simulate direct sunlight under medium tracking accuracy conditions. Measurements on these four modules revealed an increase in I_{SC} between 2.1 % and 3.3 % as measured against the unprocessed reference modules. I_{SC} is used as the main performance indicator as FF and V_{OC} remained virtually unchanged.

DIFFUSE REFLECTIVE STRING RIBBONS

The surface of a string ribbon soldered to a bus bar usually exhibits a highly specular reflective surface. These surface properties are determined in the melting and re-solidification of the tin-lead or tin-silver alloys during the soldering process. Due to the high degree of specular reflection, most of the light impinging on the bus bar leaves the module after being reflected and does not contribute to the generated. The idea behind the diffuse reflective bus bars is to create a highly diffuse reflecting surface (Lambertian reflection) on top of the soldered string ribbon. A part of the light reflected from this surface can be reflected internally at the front surface of the cover glass (see **Fig. 3**). A similar effect also increases light absorption in modules with white back sheet [*McIntosh2005*] and can be used to increase conversion efficiency in thin film crystalline modules [*Cotter1999*, *Berger2007*].

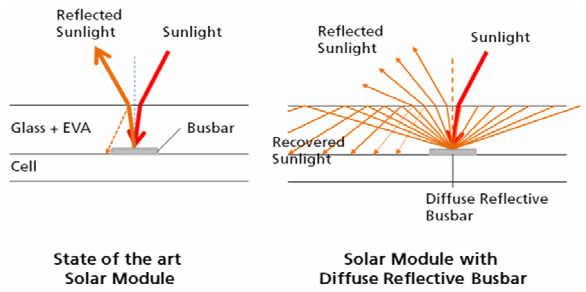

Fig. 3: *Comparison of reflection mode in a normal solar module (left) with specular reflecting bus bar and a diffuse reflective bus bar.*

We manufactured various test modules in the same process as described earlier. **Fig. 4** shows the first two manufactured modules.

Fig. 4: (Left) *Photograph of a mini-module with typical, specular reflective metallic bus wire.* ***(Right)*** *Diffuse reflective bus bar.*

Note that in this image, which is taken with a photo-flash, the dark appearance of the conventional bus bar

indicates that all light from the photo-flash is reflected away from the camera. In the module with the diffuse reflective bus bar, a significant portion of the flash light is reflected back to the camera, indicating the different reflecting behaviour.
To visualize the working principle, we used a collimated red laser beam and directed it to the string ribbon in both modules. The photographic picture of this experiment shows the light that can be recovered from the diffuse reflection at the string ribbon and the following internal reflection. (**Fig. 5**).

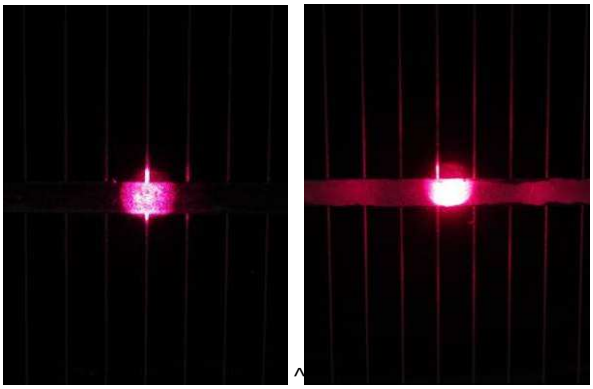

***Fig. 5**: **Left**: Collimated red laser beam impinging on a reflecting string ribbon soldered to a C-Si solar cell. Only the bright spot of the laser beam reflected mainly at the bus bar can be seen in this camera picture as a result of specular reflection. **Right**: With the laser spot impinging on the diffuse reflective string ribbon, a bright illuminated area around the central spot can be observed. This is caused by internal reflection of the diffusely scattered light.*

As can be noticed in **Fig. 5**, the reflection has a distinctive pattern. To further analyze the pattern of the internally reflected light, a string ribbon was laminated on top of a white back sheet, the rest of the module layer stack (EVA and cover glass) where the same as in the mini-modules described above.

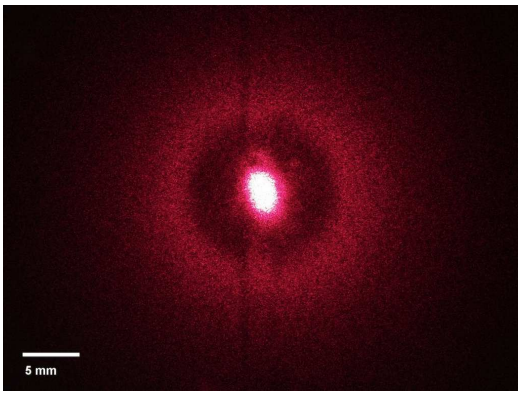

***Fig. 6**: Illumination pattern generated by a laser spot impinging on the diffuse reflective string ribbon with subsequent reflection at the front glass.*

In **Fig. 6** a dark ring is spotted between the central spot and the illuminated area. This area lies within a "dead zone", where the angle of the reflected light to the vertical axis is too low to be internally reflected.
This angle can be calculated using Snell's law of reflection

$$n1*\sin\theta_1 = n2*\sin\theta_2 \quad \text{(Eq. 1)}$$

with the symbols $n_{1,2}$, $\theta_{1,2}$ as described in **Fig. 7** (For a more detailed calculation, see [*Smestad1982*]. The critical angle is calculated by setting $\sin\theta_1$ to 90°. With the index of refraction of glass and EVA assumed to be 1.5, a critical angle of 42° is calculated using Eq . 1.

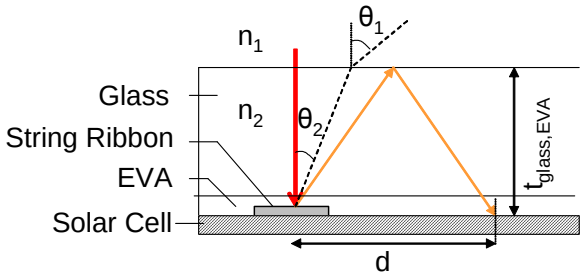

***Fig. 7**: Sketch of a ray hitting a diffusive reflective string ribbon. At the surface of the ribbon, rays with all angles of a hemisphere -0.5 π< θ_1<0.5 π are emitted. For those rays exiting the glass, the exit angle is θ_2. Index of refraction of glass n_2 is assumed to equal that of the EVA and is set to 1.5 to facilitate calculations, while the refractive index of air n_1 is set to 1.0. Total EVA and glass thickness $t_{glass,EVA}$ is 4.2 mm.*

With the critical angle in mind, the distance d of the transition between the "dead zone" and the illuminated areas as shown in **Fig. 6** and **Fig. 7** can be calculated (Eq. 2):

$$d/2 = \tan(\theta_2)*t_{glass,EVA} \quad \text{(Eq. 2)}$$

With the combined thickness of the glass and EVA layers of 4.2 mm, a distance of 5.3 mm can be calculated. This correlates well with the photographic image of **Fig. 6**. Although the camera was not calibrated for absolute irradiation measurements, it can be concluded from **Fig. 6** that the large majority of the internally reflected light hits the solar cell within 5 to 15 mm apart from the point of incidence on the string ribbon. In addition to that, the "dead zone" is not really black, as some light is also reflected into this area due to multiple internal reflections and due to Fresnel reflections at the glass surface for angles below the critical angle.
The total reflectivity of the material used is plotted in Fig. 8.

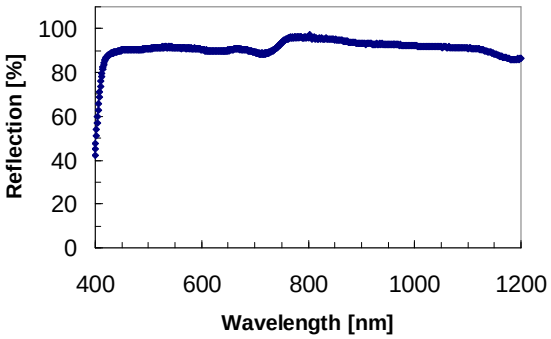

Fig. 8: Total reflection of the diffuse reflective white paint that was used for the coating of the tabbing wire as determined in a spectrophotometer.

An average reflectivity of 90.8 % was calculated from the reflection measurement presented in Fig. 8. (wavelength 400 - 1100 nm, no spectral weighting applied). Specular reflection has been determined to be < 1 % using a spectrophotometer. However, only the light reflected greater than critical angle is reflected. For a Lambertian reflector embedded in EVA and glass, [*McIntosh2005*] calculated the portion of light to be reflected above the critical angle and therefore internally reflected to amount to 56 %. The question for coated string ribbons here is to what extent the created surface could be regarded as a Lambertian reflector. To get a better indication of the angular distribution of the reflection, the reflected light was captured using a white paper. The light used for illuminating the sample was again a collimated red laser. To detect any change in the reflectivity pattern, also the angle of the laser and the string ribbon was varied between 0 and 45°. At higher incidence angles, a change in reflectivity, particularly an increase of light in the direction of specular reflection, would indicate that the surface deviates significantly from a Lambertian reflector. However, as shown in Fig. 9, even at 45° tilt angle no preferred direction of reflection could be identified, indicating a fairly good Lambertian reflector.

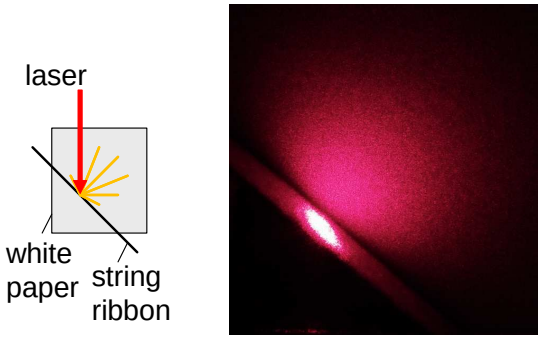

Fig. 9: Reflection pattern at an angle of 45° from a diffuse reflecting string ribbon..

To determine the effect on overall module performance, we manufactured several modules: Four mini-modules with each cell in a single module as well as two modules containing each six individually contacted cells. All in all, the data from 12 cells encapsulated in modules was evaluated, six of these cells served as a reference, the others received a diffuse reflective white coating on the bus bars after they were soldered. All cells were measured prior to module fabrication in order to eliminate the effects of differences in the cell itself. The measurements were performed on a flash simulator under STC conditions (1000 W/m2, class AAA simulator for IEC 60904-3 AM1.5g spectrum).
To increase the sensitivity of the measurements to the changes introduced by the coating of the string ribbons, four modules equipped with six string ribbons have been manufactured. In these modules, in addition to the two strings soldered to the bus bars, four string ribbons have been placed on the cell prior to lamination. Two of these modules received a white diffusive coating on all six string ribbons.

Table 1: Summary of the module measurements (SD = Standard deviation, MIN/Max: Minimum / Maximum measured value). The values represent the difference in I_{SC} of the modules having cells with coated string ribbons compared to the reference modules.

	Average increase in I_{SC}	SD	MIN	MAX
Two string ribbon mini modules	**+ 0.9 %**	0.4 %	+ 0.4 %	+ 1.4 %
Six string ribbon mini modules	+2.5 %	0.6 %	+ 2.1 %	+3.0 %

As can be seen in Table 1, the short circuit current is increased for the modules using the white coated string ribbon by an average of 0.9 %. This increase can be attributed to the increased light recovery through internal reflection. Based on this result, an increase of 2.7 % could be expected for the six string modules (3 x.0.9 %). The measured difference of 2.5 % for these modules is there fore in good agreement with the 0.9 % on the standard two string mini modules.
The gain in I_{SC} achieved by the diffusive string ribbons is lower than that of the front glass diffuser. The main reason for that is that the front glass diffuser also included the area facing the gridlines and a 2 mm space around the cells, which were left untreated in the diffusive bus bar modules. However, a coating of the fingers would not yield significant improvement: It became apparent that the screen printed grid fingers in the cells we used already showed significant diffuse reflection, in contrast to the specular reflection from the re-melted tin/lead metallization of the string ribbons. The main reason for the higher impact is therefore the principle advantage of a front side diffuser that no rays are lost due to the limitation of the critical angle of internal reflection. On the downside of a front side diffuser the need for tracking as well as possible soiling issues must be considered.

SUMMARY & CONCLUSION

Two technologies were presented which help to reduce the shading caused by the front side metallization and string ribbons in crystalline silicon solar modules. These technologies are a local laser roughening of the front surface of the module's cover glass ("front side diffuser") and the coating of the string ribbon with a diffuse reflective paint.

The front side diffuser achieves an increase in I_{SC} of 2.1 to 3.3 % under perpendicular illumination conditions. This increase indicates that the roughened surfaces can direct light away from the bus bars and grid fingers and unused areas around the cell. In conclusion, the front side diffuser is well suited to increase the efficiency for modules in installations where the modules are mounted on two axis tracking systems

The diffusive coating of the string ribbons shows good Lambertian reflection with total reflectivity exceeding 90 %. The increase in I_{SC} for one-cell modules using the coated wires was measured on a flash simulator to be 0.9 % in average. As the total bus bar shadowing is 2.6 % for this cell, about 35 % of the light impinging on the bus bars could be recovered. The light recovery is due to its principle not influenced significantly by the angle of the incident light.

We believe that particularly the diffusive bus bar is a very attractive technology due to its shear simplicity of manufacturing (applying a white paint to the soldered bus bars), the cheap raw materials used, its insensitivity to irradiance direction and last but not least the possibility of a seamless integration into the standard crystalline PV module production process.

ACKNOWLEDGEMENTS

We thank Rafal Mickiewicz for fruitful discussions on white paint properties and Biao Li, Tanja Schumacher, Carola Voelker and Matthieu Ebert for setting up the laminator and characterization equipment and Boris Rangaard for optical calculations. Funding from Fraunhofer USA is greatly acknowledged.

REFERENCES

[*Cotter1999*] J. E. Cotter, R. B. Hall, M. G. Mauk and A. M. Barnett: "Light Trapping in Silicon-Film Solar Cells with Rear Pigmented Dielectric Reflectors" Vol. 7, pp. 261-274,´1999.

[*Berger2007*] O. Berger, D. Inns, A. G. Aberle: "Commercial white paint as back surface reflector for thin-film solar cells", *Solar Energy Materials & Solar Cells* , vol. 91 pp. 1215-21, 2007.

[*McIntosh2005*] K. McIntosh, R. M. Swanson, J. E. Cotter: "A Simple Ray Tracer to Compute the Optical Concentration of Photovoltaic Modules", *Progress in Photovoltaics*, vol. 14, pp. 167-177, 2005.

[*Smestad1982*] G. Smestad and P. Hamill: "Concentration of solar radiation by white painted trasparent plates", Applied Opitcs, Vol. 21, No. 7, pp. 1298-1306, 1982.